J. Membrane Biol. 180, 21–32 (2001)
DOI: 10.1007/s002320010055

The Journal of
Membrane
Biology

Formation of Folds and Vesicles by Dipalmitoylphosphatidylcholine Monolayers Spread in Excess

R.A. Ridsdale[1,*], N. Palaniyar[1,], F. Possmayer[2], G. Harauz[1]**

[1]Department of Molecular Biology & Genetics, and Biophysics Interdepartmental Group, The University of Guelph, Guelph, Ontario, Canada, N1G 2W1

[2]Department of Obstetrics & Gynecology, The Department of Biochemistry, M.R.C. Group in Fetal and Neonatal Health and Development, The University of Western Ontario, 339 Windermere Road, London, Ontario, Canada, N6A 5A5

Received: 18 May 2000/Revised: 20 November 2000

Abstract. Lipid monolayers exist in several biological systems, including the stratum corneum of the skin, the fluid tear film of the eye, the Eustachian tube of the ear, and airway and alveolar pulmonary surfactants. In this paper, the monolayer-to-bilayer transition was studied using dipalmitoylphosphatidylcholine (DPPC) as the model. Depositing DPPC organic solvent solutions in excess at an air:buffer interface led to the formation of elongated structures which could be imaged on carbon grids by transmission electron microscopy. The structures appeared to be DPPC folds protruding into the sol. The structures were frequently ordered with respect to one another, suggesting that they arose during lateral compression due to excess DPPC and are characteristic of a type of monolayer collapse phase. In some cases, series of short folds in an extended line and series of vesicles in line or parallel to the folds were observed. This suggests the elongated folds are unstable and can resolve by forming vesicles. Fold formation occurred at defined lipid concentrations above which more vesicles were observed. Surfactant protein-A did not influence fold or vesicle formation but bound to the edges of these structures preferentially. It is concluded that DPPC monolayers can form bilayers spontaneously in the absence of surfactant apoproteins, other proteins or agents.

Key words: Bilayers — Dipalmitoylphosphatidylcholine — Collapse phase — Monolayers — Pulmonary surfactant — Surfactant protein A — Transmission electron microscopy

Introduction

Due to their amphipathic nature, phospholipids can form specific aggregates including sheetlike structures, such as monolayers and bilayers, and more complex entities, such as inverted (hexagonal$_{II}$)(H$_{II}$), nonlamellar and cuboidal phases. The contribution of lipid bilayers to biological membrane structure is well-recognized [12, 29, 34]. Although direct evidence remains limited, it has been suggested that nonbilayer lipid structures exist in biological membranes, for example, within the mitochondrial inner membrane cristae and during cell membrane fusion events [11, 15, 29, 33]. Lipid monolayers form the limiting coats of serum lipoproteins [7, 13] and have also been reported in the skin epidermis [38], the fluid tear film covering the eye [8, 22, 40], the Eustachian tube of the ear [6, 23, 24], the swim bladders of teleost fishes [5, 37] and the airspaces of the lung (i.e., airway and alveolar pulmonary surfactants) [2, 9, 28, 32, 37].

Although the existence of monolayers in biological systems is well-documented, little is known about their in vivo formation and even less about their dissolution. It appears likely that bilayer:monolayer transformations would be involved in both phenomena. The present paper describes studies attempting to elucidate potential mechanisms of lipid monolayer dissolution through transformation to other structures. Because it is the major molecular species in swimbladder, Eustachian, airway, and alveolar surfactants, all of which involve

* *Present address:* Department of Lung Biology, Hospital for Sick Children, Toronto, Ontario, Canada

** *Present address:* Department of Biochemistry, University of Oxford, Oxford, UK

Correspondence to: F. Possmayer

air:liquid interfaces, dipalmitoylphosphatidylcholine (DPPC) was adopted here as the phospholipid model.

It is generally recognized that the lateral compression of alveolar surfactant films arising during exhalation leads to ultra-low surface tensions approaching 0 mN/m at the air:liquid interface of the terminal air spaces. It is thought that surface monolayers highly enriched in DPPC are required to achieve such low tensions. For the present studies, DPPC was spread on air:buffer interfaces using organic solvents, the solvent was allowed to evaporate, and the samples were incubated at 25°C for 24 hr. Transmission electron microscopy of samples of the surface films revealed the presence of distinct surface folds and often apparently complete vesicular structures. These observations indicate that highly packed pure lipid films in the gel phase are metastable and can form three-dimensional structures, such as folds and vesicles, when surface pressure is increased.

To examine the potential effects of proteins on DPPC monolayers, surfactant protein-A (SP-A), which has been reported in Eustachian [6, 24] as well as airway and alveolar surfactants, was added to the subphase. It was observed that SP-A bound preferentially to the edges of the folds and vesicles, but this protein had no apparent effect on monolayer turnover. Hence, the monolayer to bilayer transition resulted from intrinsic properties of phospholipids and did not require the presence of proteins or other agents. However, such proteins or agents could enhance monolayer processing. The results are consistent with a mechanism involving buckling of the surface film into the subphase followed by a monolayer-to-bilayer transition and the pinching-off of vesicles.

Materials and Methods

Bovine SP-A was purified from bovine surfactant lavage by chromatography on a mannose column, as previously described [3]. The SP-A was stored at 4°C in 2 mM sodium ethylenediamine tetraacetic acid (EDTA), 5 mM HEPES-KOH (pH 7.4) at a concentration of ~200 μg/ml.

The lipids phosphatidylserine (PS), egg phosphatidylcholine (egg PC), or DPPC (Avanti Polar Lipids, Alabaster, AL) were dissolved in 1:1 chloroform:hexane at 0.45 μg/μl, unless stated. Under the standard conditions, a volume of 13 μl of HEPES-NaOH (pH 7.4), 1 mM $MgCl_2$ was added to wells approximately 4 mm in diameter and 1 mm deep, drilled into Teflon blocks. Lipid was added in a volume of 0.7 μl to the surface of the buffer. Samples were stored for approximately 24 hr at 25°C in a 15 ml petri dish containing excess buffer to minimize evaporation. Samples were then picked from the surface by a 400 mesh copper grid coated with a thin layer of carbon. After 30 sec, samples were stained with 3% uranyl formate (UF) (J.B. EM Supplies, Dorval, QC, Canada) for 1 min and excess stain was drawn off with filter paper. Other stains used were 3% uranyl acetate (UA), 5% ammonium molybdate (AM) (J.B. EM Supplies, Dorval, QC, Canada) or 2% methylamine tungstate (MT) (Marivac Halifax, NS, Canada). For platinum (Pt) shadowing, samples stained with 3% UA were permitted to dry for 20 min and then placed in a Balzers 360 M freeze fracture unit. A unidirectional shadow was applied at an angle of 20° from the top of the Pt gun with respect to the sample normal. For samples containing SP-A, the protein concentration was 20 to 60 μg/ml prior to monolayer spreading. Samples were examined by transmission electron microscopy (TEM) utilizing a JEOL JEM-100 CX [30].

Results

Monolayers of DPPC that were examined utilizing TEM showed structures with diverse surface topologies. The most distinct structure was an extended shape resembling a fold in the surface (Fig. 1). Folds were not observed in the absence of lipid or in the presence of fluid lipids, such as egg PC or PS. Other spontaneously formed vesicles and other surface topologies were observed whose appearance and physical characteristics are described later (Fig. 1). Slight dilutions of DPPC (5–10%) with PS or G_{M1} did not affect fold formation.

Various salts, including NaCl, $MgCl_2$ and $CaCl_2$ over a wide variety of concentrations, had no obvious effect on fold formation. Varying the conditions (e.g., staining times, temperature between 25 and 37°C) had little or no effect. Therefore, these parameters were not strong factors in fold formation. However, when care was taken to maintain 45°C-incubated samples at 45°C during processing, folds were not detected. When such samples were cooled to 25°C before processing, folds and vesicles were evident. This indicates folds do not form above the bilayer gel:liquid crystalline temperature transition.

The average thickness of the folds was 22.2 nm ± 5.4 nm (mean ± SD; $n = 42$) when measured through the central part of the fold, indicating little variation in thickness. Fold lengths ranged from ~10 nm to greater than 1,300 nm, and averaged 281.4 nm ± 333.3 nm ($n = 70$). Thus, fold dimensions were limited only in their width. Previous publications have demonstrated that DPPC lipid mixtures are capable of forming vesicles with rippled surfaces [4, 20, 27]. We also observed the presence of some DPPC vesicles with ripples in the absence of other structural entities (Fig. 2). Ripples had an appearance somewhat like the folds and had an average periodicity of 18.4 nm ± 0.7 nm ($n = 15$) but did not appear to be associated with folds. We occasionally observed places where it appeared that DPPC vesicles collapsed into crescent or cigar shapes as described by Williams et al. [39] (Fig. 2). Measurements of folds and other DPPC three-dimensional structures show close agreement under a variety of conditions, and therefore result from the intrinsic properties of DPPC.

Unidirectional platinum shadowing at an angle of 20° produced shadows of varied lengths (from 12 to 22 nm) indicating that the heights of the folds varied more than the widths (Fig. 3). By trigonometric calculations, the average height of the folds was 18.2 nm ± 4.6 nm ($n = 59$) through the nontapered regions of the folds. By

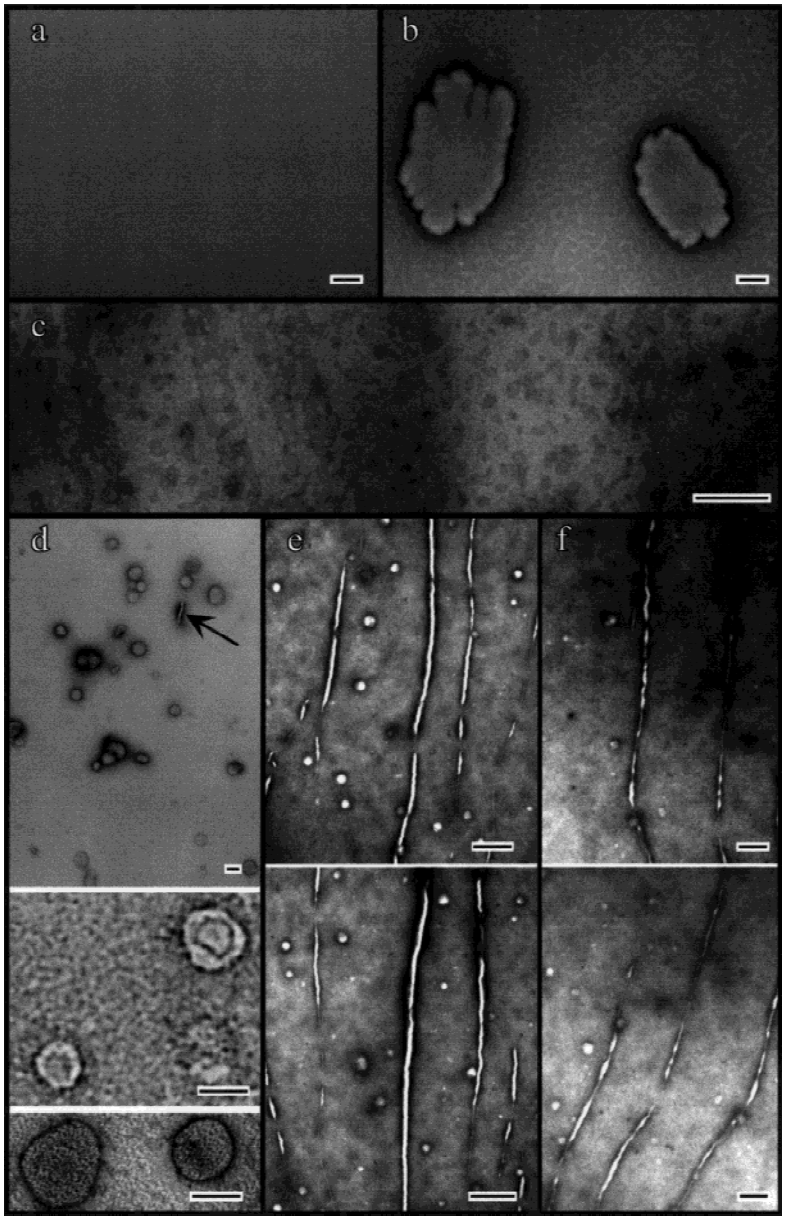

Fig. 1. A collage of lipid structures. (*a*) Micrograph of negative control sample containing no lipids, only carbon film. Very little surface character is observed. (*b*) PS (0.45 μg/μl) shows some surface "noise" and occasional vesicles. (*c*) An example of DPPC (0.45 μg/μl) surface "noise." (*d*) Examples of vesicles spontaneously formed from DPPC (0.45 μg/μl). A small fold is also present (arrow). (*e*) DPPC folds stained with 5% ammonium molybdate. (*f*) Other DPPC folds stained with 2% methylamine tungstate. Scale bar = 80 nm.

comparing the height and width of the folds (Fig. 3), it was possible to assess their general three-dimensional shape. Fold heights and widths tend to vary with each other until ~15 nm where fold widths plateaued (Fig. 3*f*). Although only small variations in thickness were seen for the central regions, the ends of many folds tapered down to termination (Fig. 3*d* and 3*e*). Thus, although the height and length could vary, the widths showed less variation. There was no evidence for depressions that would represent extensions of the monolayers into the air above the monolayer. This result suggests that folds may specifically form into the subphase.

Varying the concentration of DPPC added to the interface between 0.0025 and 25 μg/ml resulted in conspicuous changes in the numbers and appearance of both folds and vesicles (Fig. 4). At low concentrations, few folds were observed and most of these were short. As the amount of DPPC and presumably the surface pressure was increased, there was an increase in the number and length of folds. However, at higher concentrations of DPPC, there was a decrease in the number of folds but a corresponding increase in the number of vesicles. At the highest DPPC concentrations, virtually the entire field of view was filled with vesicles.

Occasionally folds displayed some order, e.g., many folds ran in parallel and/or in a line (Fig. 5). Some vesicles were aligned between folds whereas others formed a line (Fig. 6). This regular order suggested that

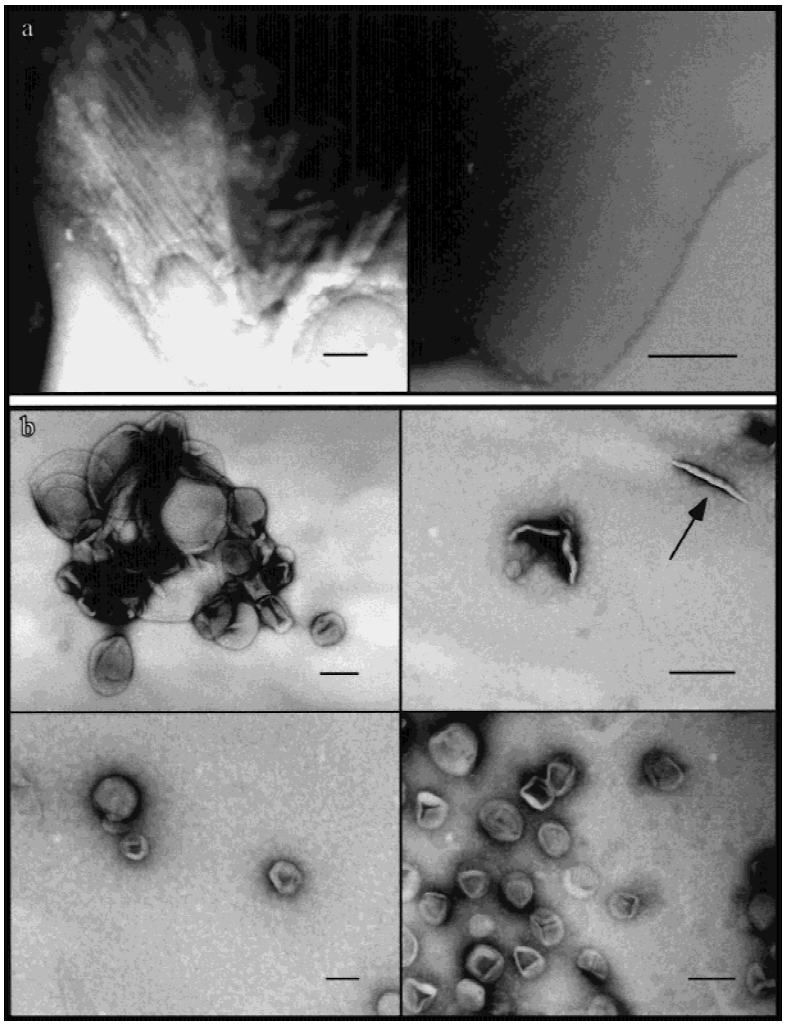

Fig. 2. A collage of DPPC vesicle structures. (*a*) Examples of ripple phase on vesicles. (*b*) Several examples of collapsed crescentlike vesicles. A fold is also present (arrow). The thickness of the fold appears similar to that of the crescent vesicle. Scale bar = 80 nm.

formation of DPPC folds, and at least some DPPC vesicles, were generated from the monolayers in a nonrandom fashion.

Surfactant protein-A, a member of the C-lectin superfamily, exhibits selective binding of DPPC [16, 17, 41]. SP-A is a large oligomeric glycoprotein composed of six trimeric subunits (monomer, 28–36 kDa; octadecamer, ~650 kDa) with an overall structure resembling a floral bouquet. The N-terminal "stalk" region consists mainly of a bundle of six collagen-like (Gly-X-Y repeats) trimers terminating in an "extra" amino acid which produces a bend or kink. The six "stem" regions are composed of further collagen-like trimers followed by short coil:coil stabilized "neck" regions. The six "flower" regions each consist of three "petal-like" glycosylated carbohydrate recognition domains (CRD). To determine whether SP-A could influence either the formation or resolution of DPPC folds, and to examine the manner in which SP-A interacted with these structures, the protein was included in the bulk phase from 20 to 60 μg/ml. DPPC was spread at those concentrations, which form folds. SP-A was found associated with grooves in the vesicles, thus clearly displaying affinity for regions with three-dimensional lipid structure. With folds and vesicles, SP-A associated primarily with the edges (Fig. 7). Vesicles formed at the monolayer surface were often decorated with SP-A. Vesicles and folds formed in the presence and absence of SP-A and therefore were not dependent on SP-A, but it was evident that the protein bound to these structures in preference to planar monolayers.

Discussion

The present investigation revealed the presence of two types of membrane structures, folds and vesicles, associated with DPPC monolayers formed from spread organic solvent. Despite a number of extensive high-resolution studies of DPPC monolayers [1, 36], to our knowledge DPPC folds as described here have not been reported in the literature, although Salesse and co-

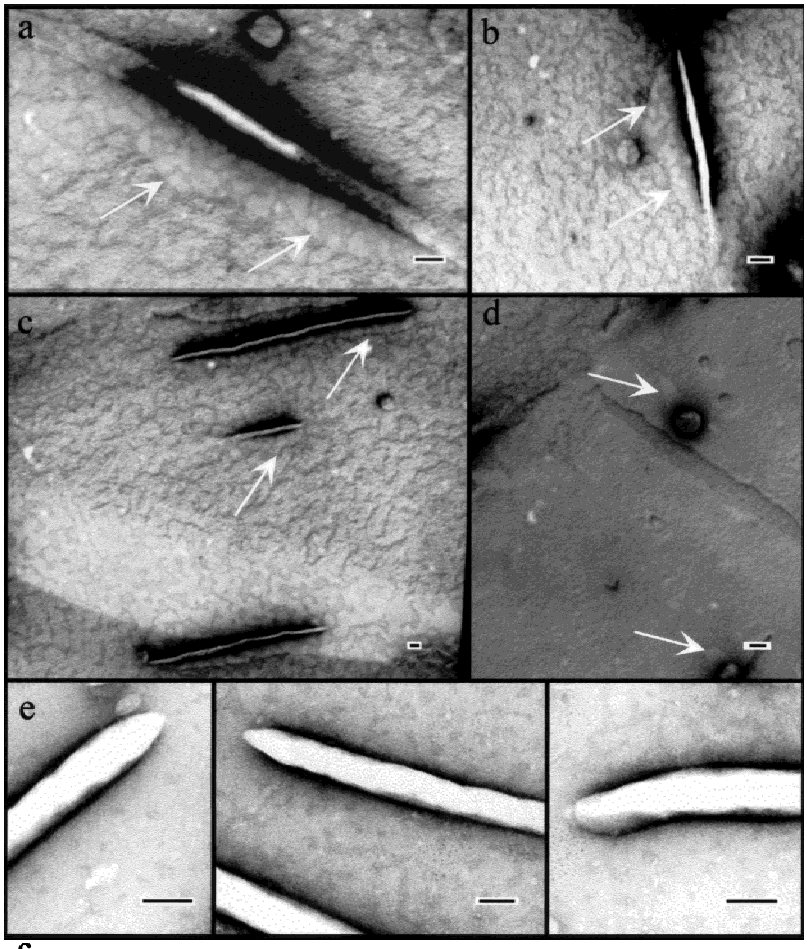

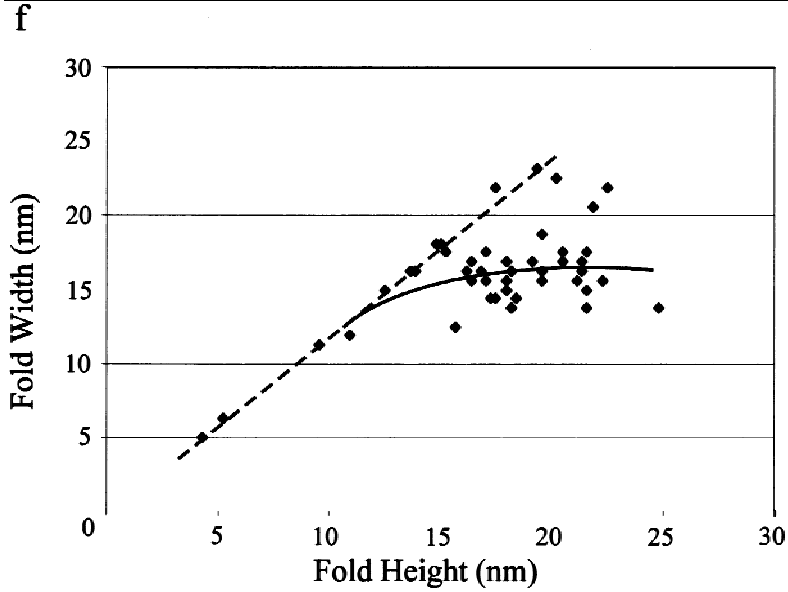

Fig. 3. Platinum shadowing of uranyl acetate-stained DPPC (0.45 μg/μl). (*a–c*) Folds display shadows indicating that they extend upwards from the support surface. Shadows rise and fall even when folds seem to be consistent in width. (*d*) A couple of vesicles displaying a shadow like that of the folds. (*e*) A collection of tapered fold ends. (*f*) Fold width related to fold height at the same point. A linear relationship is seen from 5 to ~12 nm. Although height continues to change beyond this latter value, the width remains close to the 18 nm mean. White arrows in *a–d* point to outer shadow edges. Scale bar = 15 nm.

workers have noticed similar structures (C. Salesse, U. du Québec à Trois-Riviéres, *personal communication*). Previous studies have normally used the Langmuir-Blodgett technique, where the monolayer is deposited on a substrate raised through the interface at right angles. Normally, surface pressure is maintained constant using a Langmuir-Wilhelmy surface balance, although this is not always the situation [41]. In some cases, for example, during compression of cerebronic acid and cholesterol monolayers, large ridges have been observed,

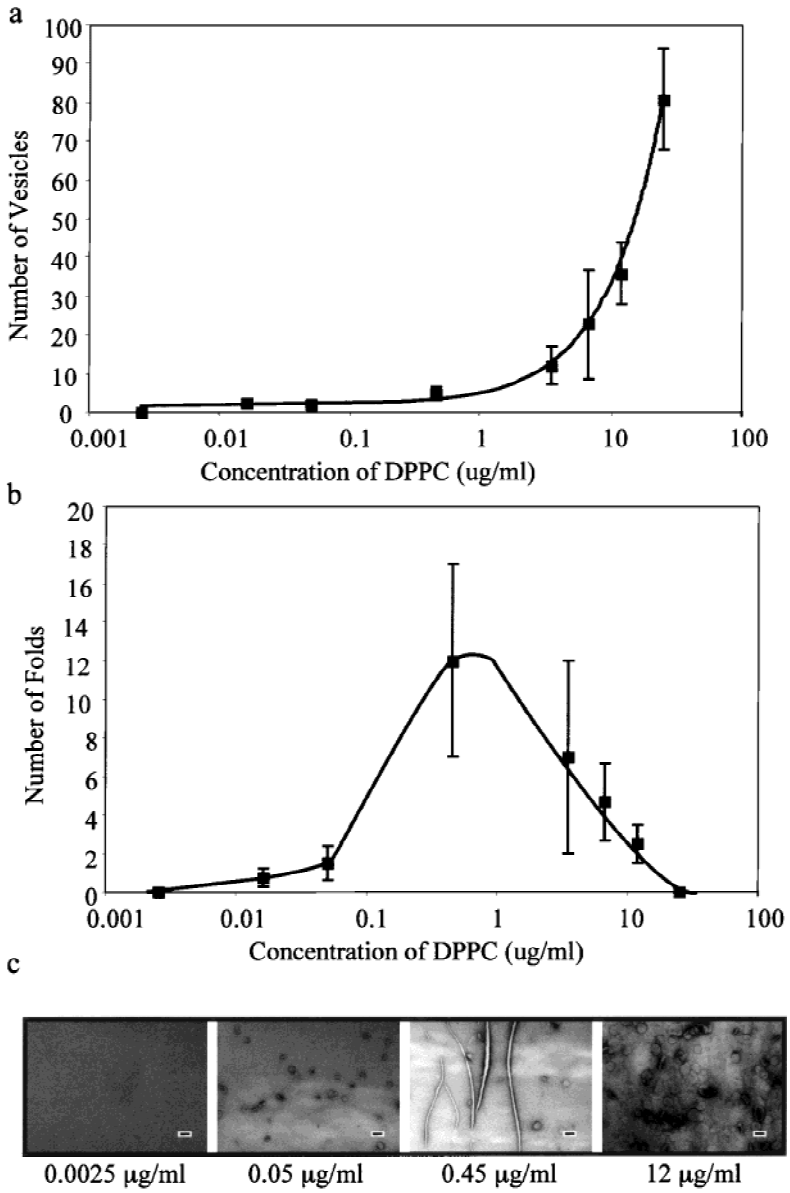

Fig. 4. Random sections of samples were evaluated regarding the presence of folds or vesicles. Data points are from 0.0025, 0.016, 0.05, 0.45, 3.5, 6.59, 12, and 25 μg/μl DPPC in the sample. (*a*) The number of vesicles found in a 200 μm^2 area at different DPPC concentrations. As the concentration of lipid increases there is a corresponding increase in the number of vesicles ($n = 4$ to 6 for each point). (*b*) The number of folds found in a 200 μm^2 area at various DPPC concentrations. Folds are most frequently observed above 0.5 μg/μl and below 6.6 μg/μl DPPC ($n = 4$ to 6 for each point). Folds decrease in frequency as vesicle numbers increase. (*c*) Some fields of view of DPPC at varied concentrations. Scale = 30 nm.

apparently formed from the overlaying of monolayer material [31]. These structures, also a kind of fold, appear distinct from the minifold reported here. In other cases, surface overcompression resulted in the appearance of flat platelike structures overriding the remaining DPPC monolayer [36]. These platelike structures do not resemble the folds observed in the present work. Vesicles were not reported in the previous studies, nor does it appear likely that vesicles could be formed from such plates which have an appearance similar to ice floes.

The reason folds have not been described previously is not known. It appears possible that minifolds could relax as the substrate is drawn up from the interface. Langmuir-Blodgett techniques normally use hydrophilic substrates, which bind the polar groups of the lipid. In the present studies, nonpolar carbon-coated grids were touched to the surface, resulting in an interaction with the hydrophobic acyl chains. Direct carbon:acyl chain interactions may be superior in preserving the elongated minifold compared to hydrophilic polar head group interactions.

The lack of previous publications describing folds led us to consider potential artifacts. The distribution of stain around the edges of the fold and vesicles indicated that these structures were present when excess stain was removed. Therefore, folds did not appear to be a drying artifact created during monolayer dehydration. Folds were observed using distinct stains and a variety of conditions, which would limit the possibility of staining artifacts.

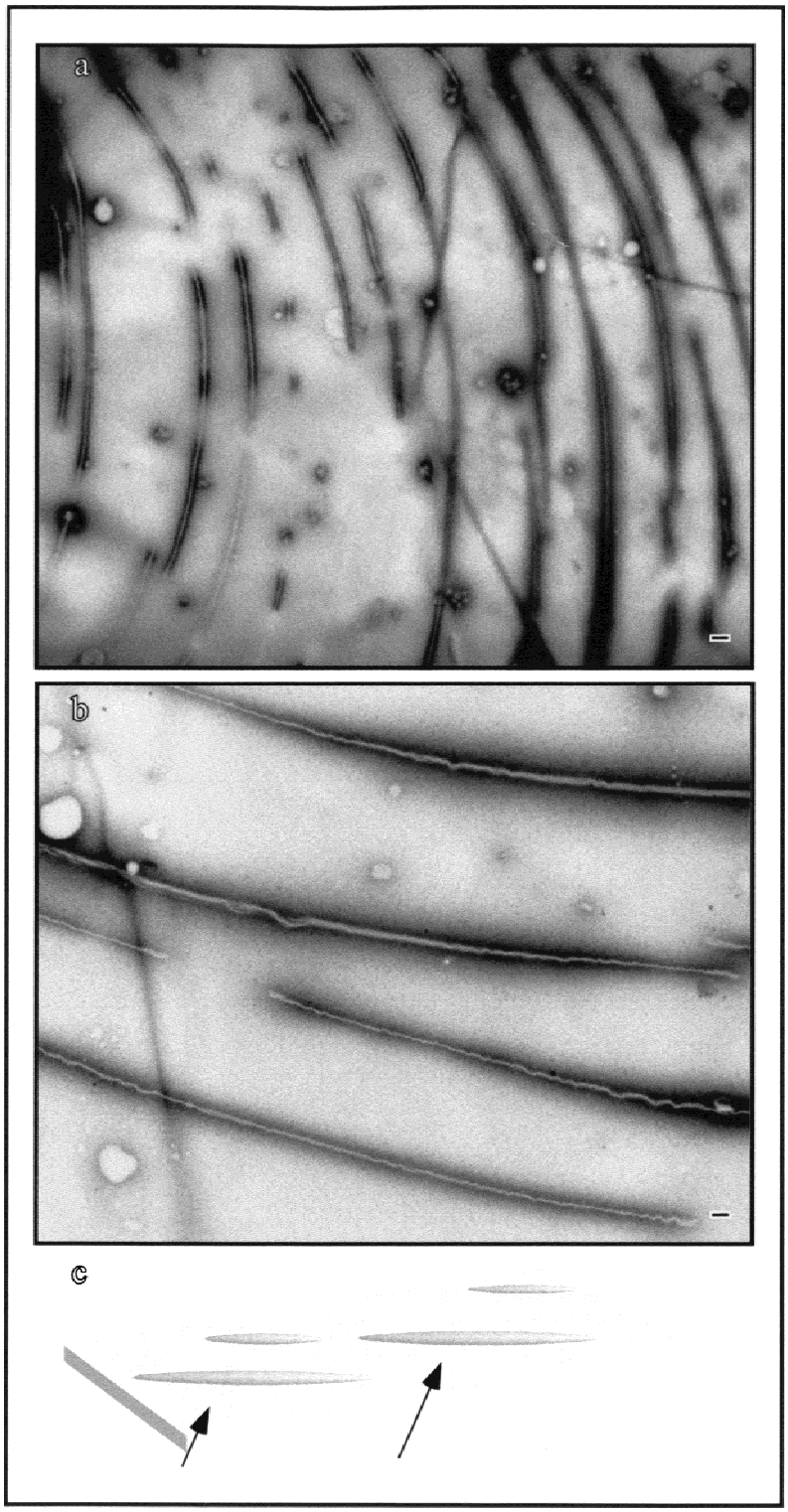

Fig. 5. (*a*) An example of DPPC folds displaying a high degree of order over the field of view. Folds often run in parallel. Some folds are seen in parallel with a more linear arrangement (*see* previous figures). (*b*) More ordered folds with one fold starting in line with another fold. (*c*) Folds likely form perpendicular to the direction of surface pressure. Fold order could be a product of that pressure in the same way that skin wrinkles from lateral force that is applied to it. Scale = 30 nm.

Examination of transferred DPPC monolayers employing ^{2}H-NMR with silanized silica beads reported the presence of highly curved structures extending from the surface [19]. Furthermore, Tajima and Gershfeld [35] obtained evidence for bilayerlike phospholipid complexes during spontaneous adsorption of DPPC and other lecithins to air-water interface near the bilayer gel-liquid phase transition temperature. The morphological nature

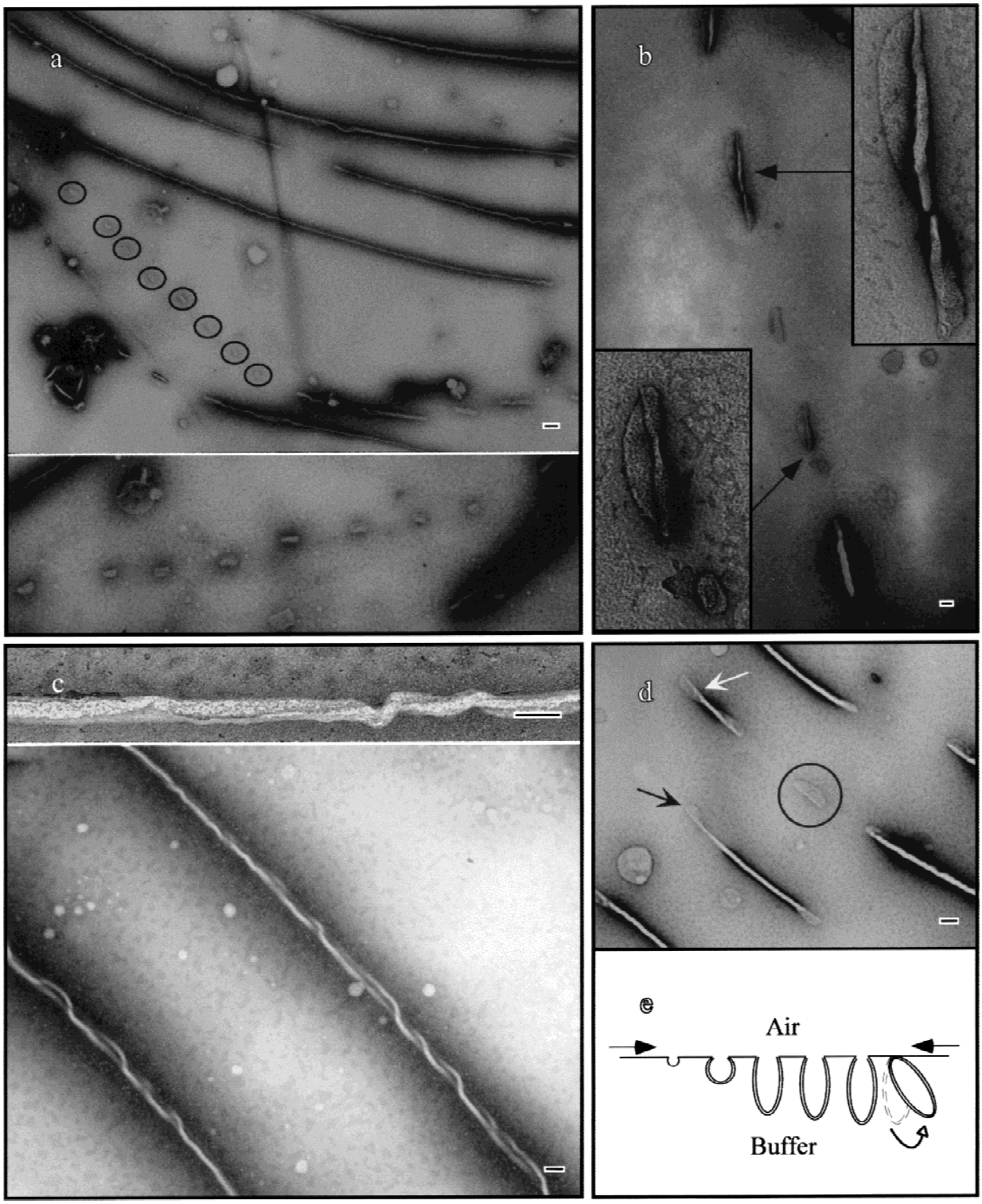

Fig. 6. (*a*) A series of eight vesicles (circled) in a row; insert is a magnification of said vesicles. These vesicles are in a line with a group of short folds and appear to have formed from the end of a fold. (*b*) Another series of 5 vesiclelike structures between two folds. Inserts are magnifications of some of the vesicles. Top right insert shows two vesicles in a crescentlike arrangement that could have twisted away from one another. (*c*) Some examples of twisted folds. (*d*) Folds with untapered ends. Some folds have vesiclelike edges rather than the tapered ends. Arrows indicate a few of these ends. White arrow indicates a fold structure that is close in appearance to (*b*) top right insert vesicles. The circle indicates a vesicle punctuating two folds. (*e*) A diagram of folds forming in profile. With increasing lateral pressure, folds extend out from the surface increasing in diameter until a maximum diameter is achieved (~18 nm). At this stage the fold may be a bilayer. The folds continue to increase in height maintaining the same width until the bilayers fuse. At this stage the folds may roll or twist, resulting in twisting of the fold structure and possibly in producing vesicles. Scale bar = 30 nm.

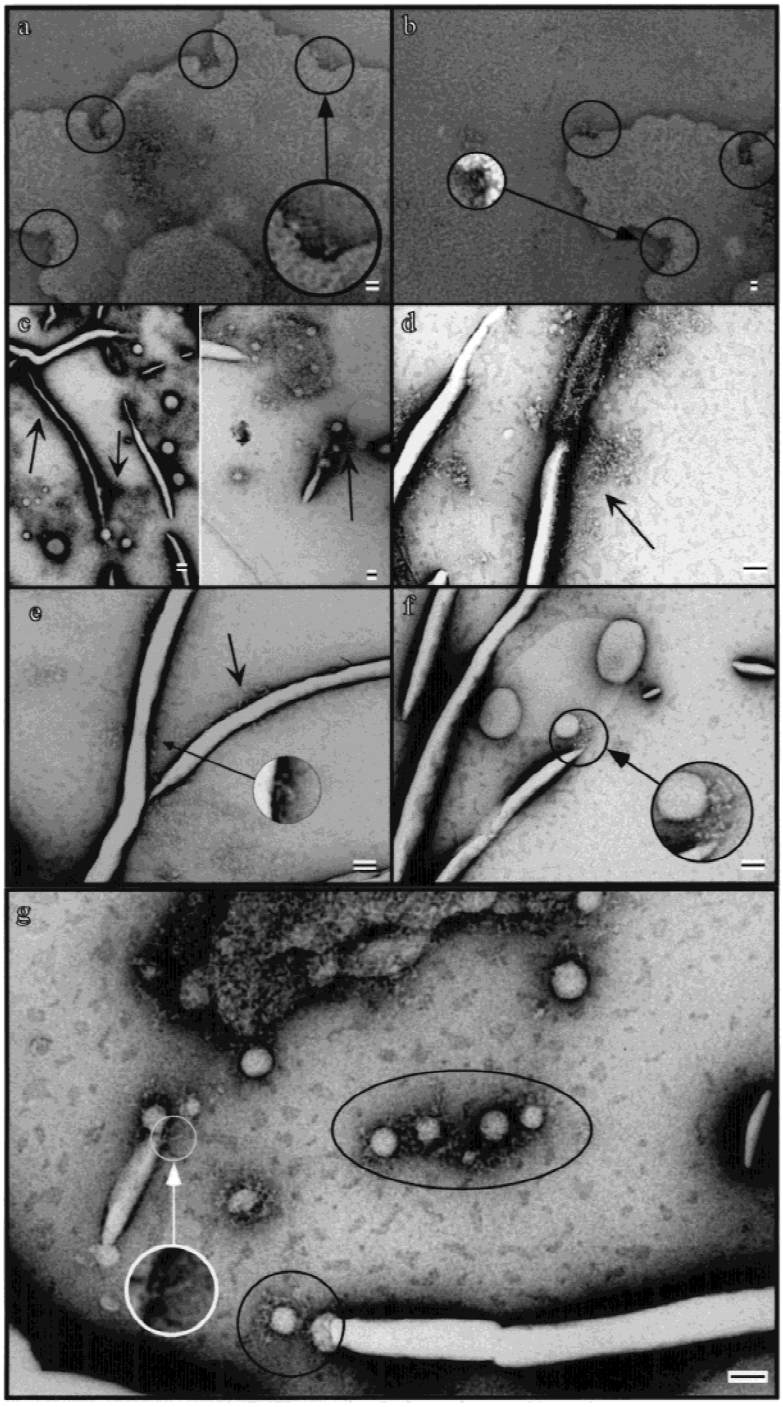

Fig. 7. Folds with SP-A. (*a* and *b*) Large egg PC vesicles with SP-A. SP-A is often found in crevices (denoted by circles) indicating that it shows a preference for curved lipid structures. (*c* and *d*) Some fields of view of DPPC folds and vesicles with SP-A. Arrows point to some SP-A seen close to or in association with DPPC structures. (*e*) Folds with associated SP-A. Insert is a magnification of a single SP-A with the tail extending away from the fold suggesting that SP-A is interacting with its head region. (*f*) The end of a DPPC fold associated with a vesicle by SP-A. Note that there is very little SP-A in areas where there is no lipid structure, suggesting that SP-A preferentially associates with these three-dimensional structures. (*g*) SP-A decorating DPPC folds and vesicles. The white circle surrounds one SP-A associated with a fold and a vesicle with its tail facing out from the ligands. The black circle surrounds another vesicle bound to a fold by SP-A. Note that the fold is twisted. The large oval comprises four vesicles bound together by SP-A. Scale bar = 15 nm.

of these structures is not known, but they could be related to the folds reported here.

Folds are observed to extend upwards from the grid surface, as characterized by the Pt shadowing (Fig. 3). Given that the monolayer was placed on the grid such that the hydrophobic tails were facing towards the underlying carbon support, the folds must have extended upwards into the area that was previously the aqueous solution. Fold lengths did not have any well-defined limitation, some being very long. The width was far more limited, having an average thickness of 22.2 nm ± 5.4 nm ($n = 42$) and in most cases, tapered down to naught.

The height and width of the folds at a particular point give an indication of the internal shape. Figure 3 relates these diameters and heights for the same locations

in a fold. The slope is close to one over a range of 0 to 15 nm. In this range the fold is close to being circular. Beyond that range the slope levels off with regard to width and the fold height continues to increase resulting in an oval (i.e., higher than wide). Interestingly, the heights of the fold increased and decreased sporadically throughout the fold as is visible from the pattern of the shadow (Fig. 3*a* and *b*).

Application of egg PC or PS to the aqueous interfaces resulted in the formation of vesicles but folds were not observed. DPPC was the only lipid tested that formed both folds and vesicles and this occurred below the bilayer phase transition. The generation of vesicles [2] and bulges [31] from monolayers has been proposed. A likely explanation for vesicle formation, in this case, is that as the organic solvent evaporates DPPC concentration in the remaining droplet increases, thus providing the driving force for monolayer and/or vesicle formation. DPPC films are relatively incompressible: a small decrease in surface area of fully occupied surfaces results in a large decrease in surface tensions. Nevertheless, although DPPC films are stable, continuous lateral pressure must inevitably result in formation of a collapse phase. The folds observed in the present study could arise from a buckling phenomenon which releases lateral surface pressure. Organic solvent remaining in the monolayer may facilitate such buckling, although folds were also observed with samples incubated at 45°C overnight before being cooled to 25°C for processing. This hypothetical model would explain formation of approximately parallel folds. This observation contrasts with the results of Tchoreloff et al. [36], who used Langmuir-Blodgett sampling and platinum shading to show that overcompression of DPPC monolayers on a Langmuir trough resulted in the formation of ice floelike plates that appeared to slide over the remaining monolayer.

Whether the folds reported in the present study represent monolayer folds in continuum with the surface monolayer, bilayers or partial bilayers is not known. The TEM pictures are images of tube walls from above, making it impossible to determine whether the walls have dimensions of monolayers (~3 nm) or bilayers (~6 nm). It appears possible that monolayer fold generation is a result of surface buckling which eventually causes the edges of the fold to come together, allowing the hydrophobic tails to interact and form a bilayer. This would result in the exposure of fatty acyl groups to be exposed to water at the leading edge. The hydrophobic effect of these exposed acyl groups should result in the rapid formation of vesicles. Folds that are ~25 nm in diameter could be hemi-tubes composed of bilayer walls which somehow resolve or fuse with monolayers at the former surface. Unresolved fold ends (arrow, Fig. 6*d*) and flattened structures in line with folds (circle, Fig. 6*d*) could represent bilayer to monolayer transitions. It is also possible that the folds are elongated tubes composed mainly or entirely of DPPC bilayers. The twists observed along some of the folds could represent the conversion of the folds into more stable vesicular structures (Fig. 6*b*). The lines of vesicles sometimes observed at the ends of folds are consistent with this interpretation. Thus folds could originate as buckled monolayers but be converted into bilayers that initially remained attached to the monolayer, but which with time would resolve into more vesicular structures (Fig. 6*e*).

It should be appreciated that other phospholipid structures could be involved in forming folds such as observed here. For example, phospholipids possessing small polar head groups can form H_{II} phase, which consists of elongated cylinders where the head groups interact with a column of water in the middle of the cylinder and the hydrophobic tails extend outwards [33]. However, H_{II} phase forms into clusters to minimize hydrophobic tail:water interactions, and H_{II} phase has never been reported for pure DPPC, which, because of the large polar head groups, preferentially forms bilayers [11]. Nevertheless, the existence of nonbilayer phospholipid structures suggests that monolayer:bilayer interconversions consistent with the TEM images reported here are theoretically possible.

The reported affinity of SP-A for DPPC [17, 41](*see* [18, 21] for review) prompted investigation of whether SP-A can affect fold formation. Previous TEM studies have shown that SP-A binds to grooves or edges of vesicles via the carbohydrate recognition domain (CRD) [25–27]. Such an interaction would be favored in tubular myelin [25, 26]. In general, more SP-A associated with these structures when calcium was present but no situations were observed where SP-A affected the number of folds or vesicles. These studies show that although SP-A binds DPPC in vesicles and folds, it is not required for and does not affect fold formation.

The interpretation that DPPC folds arise due to increased surface pressure and represent a precursor to vesicle formation has implications for the extracellular processing of alveolar surfactant. Surfactant adsorption to form a surface film is accelerated by the surfactant proteins SP-B and SP-C. SP-A also accelerates film formation, particularly in the presence of SP-B. The observation that surfactant films can reduce surface tension to near 0 mN/m during compression has been taken to indicate monolayer enrichment in DPPC. Whether the surfactant apoproteins also influence surfactant film desorption to form so-called surfactant small aggregates, which consist mainly of unilamellar vesicles, is not clear [9, 10, 32, 37]. Small aggregates arising from film desorption are taken up by type II cells for surfactant recycling or degradation. Our results indicate that SP-A alone is not sufficient to affect fold or vesicle formation. It has been proposed that a serine esterase, convertase, promotes

conversion of surfactant from the surface film to small aggregates, although the mechanism remains vague [10, 14]. The present studies emphasize that DPPC films in the gel state are inherently capable of generating folds and vesicles. This indicates that the convertase and/or other proteins can enhance, but are not required for, turnover of the surface film.

In summary, TEM has been used to examine DPPC monolayers deposited in excess on buffer using hexane: chloroform. Samples for TEM were collected by touching carbon grids to the surface of the well. TEM revealed that at certain DPPC concentrations small folds or tubes were present. These folds appeared to represent a form of collapse phase resulting from overcompression of the DPPC monolayer during deposition. The folds that extended into the sol phase from the interface were ~15 nm wide and of variable length. The folds could represent an intermediate in vesicle formation.

The authors are grateful to Dr. Kaushik Nag for helpful discussions and Mr. Kevin Inchley for providing the purified SP-A. The work was supported by grants from the Medical Research Council of Canada, the Natural Sciences and Engineering Research Council of Canada, and the Ontario Thoracic Society.

References

1. Amrein, M., von Nahmen, A., Sieber, M. 1997. A scanning force- and fluorescence light microscopy study of the structure and function of a model pulmonary surfactant. *Eur. Biophys. J.* **26:**349–357
2. Bangham, A.D. 1987. Lung surfactant: how it does and does not work. *Lung* **165:**17–25
3. Cockshutt, A.M., Weitz, J., Possmayer, F. 1990. Pulmonary surfactant-associated protein A enhances the surface activity of lipid extract surfactant and reverses inhibition by blood proteins in vitro. *Biochemistry* **29:**8424–8429
4. Czajkowsky, D.M., Huang, C., Shao, Z. 1995. Ripple phase in asymmetric unilamellar bilayers with saturated and unsaturated phospholipids. *Biochemistry* **34:**12501–12505
5. Daniels, C.B., Orgeig, S., Wood, P.G., Sullivan, L.C., Lopatko, O., Smits, A.W. 1998. The changing state of surfactant lipids: new insights from ancient animals. *Am. Zool.* **38:**305–320
6. Dutton, J.M., Goss, K., Khubchandani, K.R., Shah, C.D., Smith, R.J., Snyder, J.M. 1999. Surfactant protein A in rabbit sinus and middle ear mucosa. *Ann. Otol. Rhinol. Laryngol.* **108:**915–924
7. Ginsberg, H.N. 1998. Lipoprotein physiology. *Endocrinol. Metab. Clin. North Am.* **27:**503–519
8. Glasgow, B.J., Marshall, G., Gasymov, O.K., Abduragimov, A.R., Yusifov, T.N., Knobler, C.M. 1999. Tear lipocalins: potential lipid scavengers for the corneal surface. *Invest. Ophthalmol. Vis. Sci.* **40:**3100–3107
9. Goerke, J. 1998. Pulmonary surfactant: functions and molecular composition. *Biochim. Biophys. Acta* **1408:**79–89
10. Gross, N.J. 1995. Extracellular metabolism of pulmonary surfactant: the role of a new serine protease. *Annu. Rev. Physiol.* **57:**135–150
11. Hope, M.J., Mui, B., Ansell, S., Ahkong, Q.F. 1998. Cationic lipids, phosphatidylethanolamine and the intracellular delivery of polymeric, nucleic acid-based drugs (review). *Mol. Membr. Biol.* **15:**1–14
12. Huang, C., Li, S. 1999. Calorimetric and molecular mechanics studies of the thermotropic phase behavior of membrane phospholipids. *Biochim. Biophys. Acta* **1422:**273–307
13. Hussain, M.M. 2000. A proposed model for the assembly of chylomicrons. *Atherosclerosis* **148:**1–15
14. Inchley, K., Cockshutt, A., Veldhuizen, R., Possmayer, F. 1999. Dissociation of surfactant protein B from canine surfactant large aggregates during formation of small surfactant aggregates by in vitro surface area cycling. *Biochim. Biophys. Acta* **1440:**49–58
15. Jahn, R., Sudhof, T.C. 1999. Membrane fusion and exocytosis. *Annu. Rev. Biochem.* **68:**863–911
16. King, R.J. 1984. Lipid-apolipoprotein interactions in surfactant studied by reassembly. *Exp. Lung Res.* **6:**237–253
17. Kuroki, Y., Akino, T. 1991. Pulmonary surfactant protein A (SP-A) specifically binds dipalmitoylphosphatidylcholine. *J. Biol. Chem.* **266:**3068–3073
18. Kuroki, Y., Voelker, D.R. 1994. Pulmonary surfactant proteins. *J. Biol. Chem.* **269:**25943–25946
19. Linseisen, F.M., Hetzer, M., Brumm, T., Bayerl, T.M. 1997. Differences in the physical properties of lipid monolayers and bilayers on a spherical solid support. *Biophys. J.* **72:**1659–1667
20. Matuoka, S., Yao, H., Kato, S., Hatta, I. 1993. Condition for the appearance of the metastable P beta′ phase in fully hydrated phosphatidylcholines as studied by small-angle x-ray diffraction. *Biophys. J.* **64:**1456–1460
21. McCormack, F.X. 1998. Structure, processing and properties of surfactant protein A. *Biochim. Biophys. Acta* **1408:**109–131
22. McCulley, J.P., Shine, W. 1997. A compositional based model for the tear film lipid layer. *Tr. Am. Ophth. Soc.* **95:**79–91
23. Mira, E., Benazzo, M., DePaoli, F., Casasco, A., Calligaro, A. 1997. Surfactants of the airways. Critical review and personal research. *Acta Otorhinolaryngol. Ital.* **17:**3–16
24. Paananen, R., Glumoff, V., Hallman, M. 1999. Surfactant protein A and D expression in the porcine Eustachian tube. *FEBS Lett.* **452:**141–144
25. Palaniyar, N., Ridsdale, R.A., Hearn, S.A., Heng, Y.M., Ottensmeyer, F.P., Possmayer, F., Harauz, G. 1999. Filaments of surfactant protein A specifically interact with corrugated surfaces of phospholipid membranes. *Am. J. Physiol.* **276:**L631–L641
26. Palaniyar, N., Ridsdale, R.A., Hearn, S.A., Possmayer, F., Harauz, G. 1999. Formation of membrane lattice structures and their specific interactions with surfactant protein A. *Am. J. Physiol.* **276:**L642–L649
27. Palaniyar, N., Ridsdale, R.A., Holterman, C.E., Inchley, K., Possmayer, F., Harauz, G. 1998. Structural changes of surfactant protein A induced by cations reorient the protein on lipid bilayers. *J. Struct. Biol.* **122:**297–310
28. Perez-Gil, J., Keough, K.M.W. 1998. Interfacial properties of surfactant proteins. *Biochim. Biophys. Acta* **1408:**203–217
29. Prenner, E.J., Lewis, R.N., McElhaney, R.N. 1999. The interaction of the antimicrobial peptide gramicidin S with lipid bilayer model and biological membranes. *Biochim. Biophys. Acta* **1462:**201–221
30. Ridsdale, R.A., Palaniyar, N., Holterman, C.E., Inchley, K., Possmayer, F., Harauz, G. 1999. Cation-mediated conformational variants of surfactant protein A. *Biochim. Biophys. Acta* **1453:**23–34
31. Ries, H.E. 1983. Cholesterol and cerebronic acid interaction in a thin-film model for cell membranes. *J. Colloid and Interface Science* **92:**592–594
32. Schürch, S., Green, F.H.Y., Bachofen, H. 1998. Formation and structure of surface films: captive bubble surfactometry. *Biochim. Biophys. Acta* **1408:**180–202
33. Siegel, D.P., Epand, R.M.. 1997. The mechanism of lamellar-to-inverted hexagonal phase transitions in phosphatidylethanolamine:

Implications for membrane fusion mechanisms. *Biophys. J.* **73:**3089–3111

34. Somerharju, P., Virtanen, J.A., Cheng, K.H. 1999. Lateral organization of membrane lipids. The superlattice view. *Biochim. Biophys. Acta* **1440:**32–48
35. Tajima, K., Gershfeld, N.L. 1985. Phospholipid surface bilayers at the air-water interface. I. Thermodynamic properties. *Biophys. J.* **47:**203–209
36. Tchoreloff, P., Gulik, A., Denizot, B., Proust, J.E., Puisieux, F. 1991. A structural study of interfacial phospholipid and lung surfactant layers by transmission electron microscopy after Blodgett sampling: influence of surface pressure and temperature. *Chem. Phys. Lipids* **59:**151–165
37. Veldhuizen, R., Nag, K., Orgeig, S., Possmayer, F. 1998. The role of lipids in pulmonary surfactant. *Biochim. Biophys. Acta* **1408:**90–108
38. Wertz, P.W. 1997. Integral lipids of hair and stratum corneum. *Exs.* **78:**227–237
39. Williams, M.C., Hawgood, S., Hamilton, R.L. 1991. Changes in lipid structure produced by surfactant proteins SP-A, SP-B, and SP-C. *Am. J. Respir. Cell Mol. Biol.* **5:**41–50
40. Wong, H., Fatt, I., Radke, C.J. 1996. Deposition and thinning of the human tear film. *J. Colloid Interface Sci.* **184:**44–51
41. Yu, S.H., Possmayer, F. 1996. Effect of pulmonary surfactant protein A and neutral lipid on accretion and organization of dipalmitoylphosphatidylcholine in surface films. *J. Lipid Res.* **37:**1278–1288